

# Third-Order Møller-Plesset Perturbation Theory Made Useful? Choice of Orbitals and Scaling Greatly Improves Accuracy for Thermochemistry, Kinetics and Intermolecular Interactions

Luke W. Bertels,<sup>†</sup> Joonho Lee,<sup>†</sup> and Martin Head-Gordon<sup>\*,†</sup>

<sup>†</sup>*Department of Chemistry, University of California, Berkeley, California 94720, USA.*

<sup>‡</sup>*Chemical Sciences Division, Lawrence Berkeley National Laboratory, Berkeley, California 94720, USA.*

E-mail: [mhg@cchem.berkeley.edu](mailto:mhg@cchem.berkeley.edu)

## Abstract

We develop and test methods that include second and third-order perturbation theory (MP3) using orbitals obtained from regularized orbital-optimized second-order perturbation theory,  $\kappa$ -OOMP2, denoted as MP3: $\kappa$ -OOMP2. Testing MP3: $\kappa$ -OOMP2 shows RMS errors that are 1.7 to 5 times smaller than MP3 across 7 data sets. To do still better, empirical training of the scaling factors for the second- and third-order correlation energies and the regularization parameter on one of those data sets led to an unregularized scaled ( $c_2 = 1.0$ ;  $c_3 = 0.8$ ) denoted as MP2.8: $\kappa$ -OOMP2. MP2.8: $\kappa$ -OOMP2 yields significant additional improvement over MP3: $\kappa$ -OOMP2 in 4 of 6 test data sets on thermochemistry, kinetics, and noncovalent interactions. Remarkably, these two methods outperform coupled cluster with singles and doubles in 5 of the 7 data sets considered, at greatly reduced cost (no  $\mathcal{O}(N^6)$  iterations).

Single-reference second-order Møller-Plesset perturbation theory (MP2) is among the most popular correlated wavefunction methods in electronic structure theory, in part due to its economical  $\mathcal{O}(N^5)$  scaling, where  $N$  is the basis set size.

$$E_{MP2} = -\frac{1}{4} \sum_{ijab} \frac{|\langle ij || ab \rangle|^2}{\Delta_{ij}^{ab}} \quad (1)$$

Equation (1) gives the correlation energy for MP2, where  $i, j, \dots$  represent occupied molecular orbitals,  $a, b, \dots$  represent virtual molecular orbitals, and  $\Delta_{ij}^{ab} = \varepsilon_a + \varepsilon_b - \varepsilon_i - \varepsilon_j$  is the (non-negative) energy denominator. The resolution-of-identity (RI) technique applied to MP2 has allowed for a much more widespread use due to the reduction of the prefactor in the overall computational cost of the algorithm.<sup>1,2</sup>

Orbital-optimized MP2 (OOMP2) methods were developed to improve the performance of MP2 for energies and other properties.<sup>3–5</sup> For systems where the unrestricted Hartree-Fock (UHF) reference exhibits spin-contamination (artificial spin-symmetry breaking), the use of these reference orbitals can lead to catastrophic performance of MP2.<sup>6–9</sup> OOMP2 can also be thought of as a relatively inexpensive way to approximate Brückner orbitals.<sup>3</sup> Orbital optimization at the MP2 level often reduces the level of spin-contamination and improves energetics.<sup>3,4,10</sup>

Despite the benefits of OOMP2 described above, there are several unsatisfying characteristics of the method that limit its applicability. Orbital optimization at the MP2 level can produce divergent energy contributions due to small energy denominators. This is often observed when stretching bonds and leads to significant underestimation of harmonic vibrational frequencies.<sup>11</sup> OOMP2 also often fails to continuously transition from spin-restricted (R) to spin-unrestricted (U) solutions even when the U solution is lower in energy.<sup>12</sup> A continuous R to U transition requires a Coulson-Fischer point where the lowest eigenvalue of the R to U stability Hessian becomes zero.<sup>13</sup> Resolution of this issue is necessary to reach the proper dissociation limit for bond-breaking curves.

Our group has attempted to remedy these issues of OOMP2 through use of regularization to prevent divergence of the energy due to small energy denominators. The first of these approaches was to shift the energy denominator by a constant factor,  $\delta$ , so that  $\Delta_{ij}^{ab} \leftarrow \Delta_{ij}^{ab} + \delta$ .<sup>11</sup> This simple form was able to resolve the two issues with OOMP2 described above. The regularization parameter,  $\delta$ , both prevents the energy expression from diverging and damps the correlation energy contribution from MP2, leading the method to more closely resemble the continuous R to U transition seen in the HF reference. Unfortunately, in the case of scaled opposite spin OOMP2 (SOS-OOMP2), Razban et al.<sup>14</sup> found the values of  $\delta$  that could restore Coulson-Fischer points were very large and consequently led to poor performance on problems that are normally well-treated by MP2.

Recently, two of us<sup>15</sup> developed explored two new classes of orbital energy dependent regularizers for OOMP2, of which the most promising is denoted as  $\kappa$ -OOMP2. In  $\kappa$ -OOMP2, the matrix elements associated with small denominators are damped such that:

$$E_{MP2}(\kappa) = -\frac{1}{4} \sum_{ijab} \frac{|\langle ij || ab \rangle|^2}{\Delta_{ij}^{ab}} \left(1 - e^{-\kappa(\Delta_{ij}^{ab})}\right)^2 \quad (2)$$

Unlike the case of  $\delta$ -OOMP2, for  $\kappa$ -OOMP2 the unregularized energy expression is recovered for large energy denominators, and in the limit of small energy denominators, the correlation energy contributions are zero. Regularization parameters of  $\kappa \leq 1.5E_h^{-1}$  were found to restore Coulson-Fischer points for hydrogen, ethane, ethene, and ethyne bond-breaking curves.  $\kappa$  was trained on the W4-11 set to suggest a value for general application.<sup>16</sup> The result,  $\kappa = 1.45E_h^{-1}$ , proved robust to further testing on the RSE43<sup>17</sup> and TA13<sup>18</sup> sets, and defines  $\kappa$ -OOMP2 as a replacement for OOMP2. Complex restricted (cR) and complex general (cG) orbital extensions of  $\kappa$ -OOMP2 have also been used to interrogate singlet biradicaloids<sup>19</sup> and the nature of symmetry breaking in fullerenes,<sup>20</sup> respectively.

The success and ubiquity of MP2 and OOMP2 have led several research groups to develop modified second-order methods aimed at improving energetics. Notable examples are spin-

component-scaled MP2 (SCS-MP2)<sup>21–26</sup> and orbital optimized SCS-MP2 (SCS-OOMP2)<sup>3,4</sup> methods, which weight correlation contributions coming from same-spin and opposite-spin pairs of electrons differently. These techniques have also been applied to the second-order correlation contribution in several double-hybrid density functionals.<sup>27–31</sup> A subset of these methods, scaled-opposite-spin MP2 (SOS-MP2)<sup>22,24,26</sup> and SOS-OOMP2,<sup>3</sup> are notable in that they can be implemented via an overall  $\mathcal{O}(N^4)$  computational cost. Another example are the attenuated MP2 methods that partially cancel basis set superposition errors with errors in MP2 itself to yield improved intermolecular interaction energies in finite basis sets.<sup>32–35</sup>

Inclusion of higher-order terms in the perturbative expansion provides another approach to improve energetics from MP2.

$$\begin{aligned}
E_{MP3} = & \frac{1}{8} \sum_{ijabcd} (t_{ij}^{ab})^* \langle ab||cd \rangle t_{ij}^{cd} \\
& + \frac{1}{8} \sum_{ijklab} (t_{ij}^{ab})^* \langle kl||ij \rangle t_{kl}^{ab} \\
& - \sum_{ijkabc} (t_{ij}^{ab})^* \langle kb||ic \rangle t_{kj}^{ac}
\end{aligned} \tag{3}$$

Equation (3) gives the third-order Møller-Plesset (MP3) contribution to the correlation energy in the spin-orbital basis. MP3 formally scales as  $\mathcal{O}(N^6)$  with basis set size, and describes the leading interaction of first-order pair-correlations,  $t_{ij}^{ab}$ , with each other. However, despite the higher compute cost, MP3 only modestly improves MP2 results (e.g. see data presented later). In passing we note that it is possible to utilize separable density fitting techniques such as tensor hypercontraction to achieve the quartic scaling ( $\mathcal{O}(N^4)$ ) MP3 (and also MP2) energy evaluation.<sup>36</sup>

Grimme<sup>37</sup> developed a spin-component scaled MP3 (SCS-MP3) method that improved ground state energies over SCS-MP2 for reaction energies, atomization energies, ionization energies, and stretched geometries. This method applied an overall third-order correlation

energy scaling factor of 0.25 in addition to the scaling factors same-spin and opposite-spin components. For weak noncovalent interactions, application of MP3 has failed to substantially improve binding energies as compared to MP2.<sup>25,37–42</sup> Hobza and coworkers<sup>40–42</sup> proposed scaling the third-order correlation energy to interpolate between the MP2 and MP3, leading to the development of MP2.5 and MP2.X, in order to improve binding energies for noncovalent interactions. Following these successes, Bozkaya and coworkers<sup>10,43–45</sup> developed OOMP3 and OOMP2.5 and evaluated the performance of these methods on thermochemistry, kinetics, and noncovalent interactions. OOMP2.5 was shown to outperform coupled cluster theory with single and double excitations (CCSD)<sup>46,47</sup> on reaction energies and barrier heights<sup>10</sup> and perform comparably to couple cluster with single, double, and perturbative triple excitations [CCSD(T)]<sup>48</sup> for noncovalent interactions.<sup>44</sup> These are very promising results.

Following the recent success of regularized OOMP2 in treating inherent problems in OOMP2, we decided to explore the use of  $\kappa$ -OOMP2 orbitals at the MP3 level. At the same time, we wanted to see if  $\kappa$  regularization in MP3 could improve the overall energetics. Beginning from  $\kappa$ -OOMP2 would allow this method to avoid energy divergences caused by small energy denominators.<sup>15</sup> In  $\kappa$ -OOMP2, damping of the two-electron integrals leads to the following expression for the  $t$ -amplitudes:

$$t_{ij}^{ab}(\kappa) = -\frac{\langle ab|ij\rangle}{\Delta_{ij}^{ab}} \left(1 - e^{-\kappa\Delta_{ij}^{ab}}\right). \quad (4)$$

Inserting Equation (4) into Equation (3) we arrive at a regularized third-order correlation energy expression,  $E_{MP3}(\kappa)$ . Our first candidate ansatz involved calculating the  $\kappa$ -OOMP2 energy and applying a scaled single-shot  $E_{MP3}(\kappa)$  correction.

$$E_c(\kappa_2, \kappa_3, c_3) = E_{MP2}(\kappa_2) + c_3 E_{MP3}(\kappa_3) \quad (5)$$

As a second, more alternative form, we considered using  $\kappa$ -OOMP2 (with  $\kappa = 1.45E_h^{-1}$ ) as

a method to generate orbitals for use in correlated calculations containing second and third order energies which could then be independently regularized and/or scaled:

$$E_c(\kappa, c_2, c_3) = c_2 E_{MP2}(\kappa) + c_3 E_{MP3}(\kappa) \quad (6)$$

The non-Brillouin singles contribution is included at second-order as  $\kappa$ -OOMP2 does not obey the Brillouin theorem. For simplicity (and ease of implementation), we do not include a non-Brillouin singles contribution at third-order.

We trained both energy functionals on the non-multireference (non-MR) subset of the W4-11 thermochemistry data set.<sup>16</sup> We excluded the MR points in the set from the training data because the single reference methods we are investigating should not be able to describe these systems adequately. Reference data were computed using CCSD(T).<sup>48</sup> Both reference and training calculations were performed using the aug-cc-pVTZ (aVTZ) basis set<sup>49-51</sup> and the corresponding RI basis<sup>52,53</sup> without the frozen core approximation. All calculations were performed in a development version of Q-Chem.<sup>54</sup>

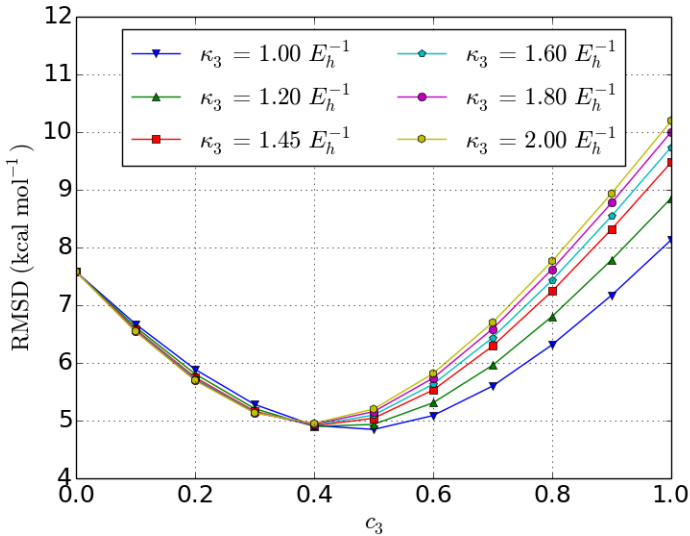


Figure 1: Scans of the root mean square deviation on the non-MR subset of the W4-11 thermochemical dataset, in  $\text{kcal mol}^{-1}$ , for the scaled, two regularization parameter correlation energy functional given in Equation 5. We fix  $\kappa_2 = 1.45 E_h^{-1}$ . All calculations use the aVTZ basis; CCSD(T) is used for the reference values.

Figure 1 presents the root mean square deviations (RMSD) for scans of the  $\kappa_3$  and  $c_3$  parameters in the first model, as given by Equation 5. Overall, we see that stronger regularization at third-order (smaller  $\kappa_3$ ) serves to lower the error on the training set. For  $\kappa_3 = 1.00 E_h^{-1}$ , the optimal scaling parameter for the third-order regularized correlation energy is 0.5 for a RMSD of 4.85 kcal mol<sup>-1</sup>. If instead one applies the same regularization parameter ( $\kappa = 1.45 E_h^{-1}$ ) at second- and third-order, we find an optimal scaling parameter for the third order correlation energy of  $c_3 = 0.4$  with a RMSD of 4.91 kcal mol<sup>-1</sup>. We note that  $c_3 = 0.0$  corresponds to  $\kappa$ -OOMP2 with a RMSD of 7.58 kcal mol<sup>-1</sup>. Inclusion of scaled, regularized third-order correlation energy contributions reduces the RMSD of  $\kappa$ -OOMP2 by more than 2.5 kcal mol<sup>-1</sup>, which is useful but not dramatic.

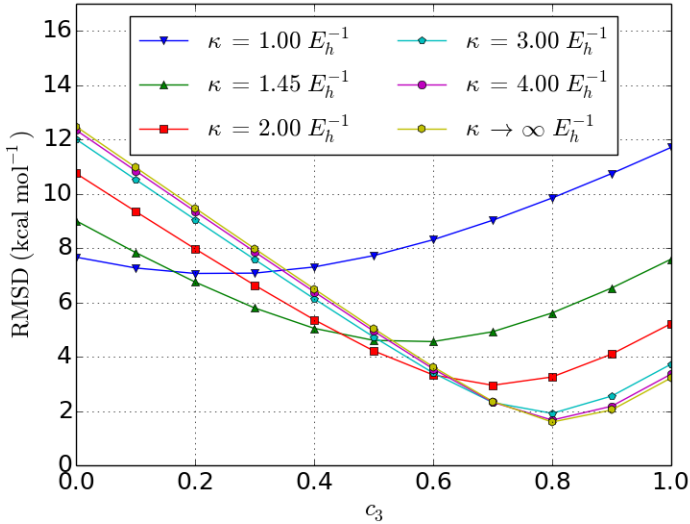


Figure 2: Scans of the root mean square deviation on the non-MR subset of the W4-11 thermochemical dataset, in kcal mol<sup>-1</sup>, for the regularized, second- and third-order correlation energy functional given in Equation 6. The optimal value of  $c_2$  was found to be 1.0 for all  $\kappa$  values plotted. SCF references were generated via  $\kappa$ -OOMP2 orbital optimization. The basis set used was aVTZ. Reference values are calculated at the CCSD(T)/aVTZ level of theory.

Turning to the second form we considered, Figure 2 presents the RMSDs for scans of the  $\kappa_3$  and  $c_3$  parameters in Equation 6 with  $c_2 = 1.0$  (the optimal value for all  $\kappa$  values plotted). For this ansatz, we see that the error relative to CCSD(T)/aVTZ is driven down quite

dramatically by weakening the regularization (increasing  $\kappa$ ). Indeed, perhaps surprisingly, we find that computing energies with unregularized MP2 and scaled unregularized MP3 provides the lowest error. In this case, the optimal  $c_3$  parameter was found to be 0.8 and yields a RMSD of only 1.59 kcal mol<sup>-1</sup>, which is close to chemical accuracy. We also observe that increasing the regularization strength decreases the optimal fraction of regularized third-order correlation energy. Impressed with the performance on this set, we chose this method, which we denote as MP2.8: $\kappa$ -OOMP2, as our candidate for further evaluation.

In order to assess the transferability of MP2.8: $\kappa$ -OOMP2, we tested its performance on a series of benchmarks sets meant to encompass a variety of main group bonded and non-bonded interactions: the non-MR subset of the W4-11 set<sup>16</sup> (the training set), the BH76RC set,<sup>55-57</sup> the RSE43 set,<sup>17,58</sup> the HTBH38 set,<sup>56</sup> the NHTBH38 set,<sup>57</sup> the TA13 set,<sup>18</sup> and the A24 set.<sup>59</sup> We compare the performance of MP2.8: $\kappa$ -OOMP2 against an unscaled version of the method (MP3: $\kappa$ -OOMP2), CCSD,<sup>46,47</sup> MP2.5,<sup>40</sup> MP3,  $\kappa$ -OOMP2,<sup>15</sup> OOMP2, and MP2. Details of the computations (aVTZ basis, CCSDT(T) reference, no frozen core) are the same as given previously.

Table 1 presents the the RMSDs, mean signed deviations (MSD), minimum deviations (MIN), and maximum deviations (MAX), in kcal mol<sup>-1</sup>, for the non-MR subset of the W4-11 set (the training set). This set includes atomization energies (TAE140), bond dissociation energies (BDE99), heavy atom transfer energies (HAT707), nucleophilic substitution reaction energies (SN13), and isomerization energies (ISOMERIZATION20).<sup>16</sup> We see that CCSD has a RMSD of 4.94 kcal mol<sup>-1</sup> and a MSD of 1.49 kcal mol<sup>-1</sup>. MP2, MP2.5 and MP3 on top of UHF orbitals yields RMSDs of 11.99, 8.97, and 9.24 kcal mol<sup>-1</sup>, respectively. The use of  $\kappa$ -OOMP2 optimized orbitals for the computation of the MP3 energy reduces the error over the use of UHF orbitals by a remarkably large factor of 3. MP2.8/ $\kappa$ -OOMP2 yields a RMSD of 1.59 kcal mol<sup>-1</sup> and a MSD of -0.45 kcal mol<sup>-1</sup>, which is 6 times smaller than MP3. This is also an improvement on  $\kappa$ -OOMP2 by a factor of 4. Also remarkably, both third-order methods computed using  $\kappa$ -OOMP2 optimized orbitals outperform CCSD on this data set.

Table 1: Root mean square deviation, mean signed deviation, minimum deviation, and maximum deviation, in  $\text{kcal mol}^{-1}$  for the non-MR subset of the W4-11 set.

Method	RMSD	MSD	MIN	MAX
CCSD	4.94	1.49	-8.60	20.34
MP2.8: $\kappa$ -OOMP2	1.59	-0.45	-5.83	5.24
MP3: $\kappa$ -OOMP2	3.22	0.33	-8.12	14.63
MP2.5	8.97	-2.85	-40.24	24.87
MP3	9.24	-0.80	-38.57	31.66
$\kappa$ -OOMP2	7.58	-3.14	-38.94	13.56
OOMP2	10.82	-3.50	-48.81	17.87
MP2	11.99	-4.90	-51.14	27.28

To validate the performance for thermochemistry outside of the training set, we tested MP2.8: $\kappa$ -OOMP2 on the BH76RC<sup>55–57</sup> and RSE43<sup>17,58</sup> sets. The BH76RC set contains reaction energies for 30 reactions involved in the HTBH38 and NHTBH38 sets.<sup>55–57</sup> On this set MP2.8: $\kappa$ -OOMP2 outperforms all other methods surveyed with an RMSD of 0.84  $\text{kcal mol}^{-1}$  and a MSD of -0.14  $\text{kcal mol}^{-1}$ . MP3: $\kappa$ -OOMP2 also performs very well. Of the  $\mathcal{O}(N^5)$  methods,  $\kappa$ -OOMP2 provides the lowest RMSD while MP2 provides the lowest overall MSD. The largest absolute error using the canonical MP methods is for the  $\text{H} + \text{F}_2 \longrightarrow \text{HF} + \text{H}$  reaction energy. This can be traced back to spin-contamination at the UHF level in the case of  $\text{F}_2$  with a  $\langle S^2 \rangle$  of 0.293. Both  $\kappa$ -OOMP2 and MP2.8: $\kappa$ -OOMP2 show significant improvement on this case with errors of 1.425  $\text{kcal mol}^{-1}$  and 0.536  $\text{kcal mol}^{-1}$ , respectively. MP2.8: $\kappa$ -OOMP2 improves upon  $\kappa$ -OOMP2 in all but two cases in this set.

Table 2: Root mean square deviation, mean signed deviation, minimum deviation, and maximum deviation, in  $\text{kcal mol}^{-1}$ , for the BH76RC set.

Method	RMSD	MSD	MIN	MAX
CCSD	1.905	-0.645	-7.175	1.977
MP2.8: $\kappa$ -OOMP2	0.835	-0.143	-1.465	1.534
MP3: $\kappa$ -OOMP2	1.574	-0.437	-6.213	1.228
MP2.5	4.625	-0.536	-21.407	9.904
MP3	4.511	-0.975	-21.604	4.232
$\kappa$ -OOMP2	4.220	-0.276	-9.763	11.856
OOMP2	5.524	0.836	-10.010	20.496
MP2	6.341	-0.098	-21.211	15.577

Table 3 contains benchmark results for the RSE43 set. The RSE43 set contains reaction energies for hydrogen abstraction from hydrocarbons by a methyl radical.<sup>17,58</sup> For this set we see MP2.8: $\kappa$ -OOMP2, with an RMSD of 0.63 kcal mol<sup>-1</sup> and a MSD of -0.54 kcal mol<sup>-1</sup>, performs slightly worse than CCSD and MP3: $\kappa$ -OOMP2. However the RMSD is still almost 4 times smaller than MP3. MP2.8: $\kappa$ -OOMP2, MP3: $\kappa$ -OOMP2, and OOMP2 all underestimate the reaction energies on average. For the  $\mathcal{O}(N^5)$  methods,  $\kappa$ -OOMP2 outperforms OOMP2 and MP2 both in terms of RMSD and MSD. Several species in the set exhibit spin contamination, leading to failures of the canonical MP methods.

Table 3: Root mean square deviation, mean signed deviation, minimum deviation, and maximum deviation, in kcal mol<sup>-1</sup>, for the RSE43 set.

Method	RMSD	MSD	MIN	MAX
CCSD	0.446	0.316	-0.815	0.973
MP2.8: $\kappa$ -OOMP2	0.634	-0.538	-1.726	0.050
MP3: $\kappa$ -OOMP2	0.521	-0.416	-1.550	-0.002
MP2.5	3.234	1.907	0.061	12.899
MP3	2.433	1.563	0.109	9.361
$\kappa$ -OOMP2	0.476	0.119	-0.964	1.020
OOMP2	0.922	-0.607	-2.261	0.478
MP2	4.099	2.252	-0.028	16.445

To evaluate the performance of MP2.8/ $\kappa$ -OOMP2 on kinetics, we tested it on the HTBH38<sup>56</sup> and NHTBH38<sup>57</sup> data sets. The HTBH38 set contains forward and reverse barrier heights for 19 hydrogen transfer reactions.<sup>56</sup> Results for this set are presented in Table 4. On this set MP2.8: $\kappa$ -OOMP2 (and MP3: $\kappa$ -OOMP2) outperform the other methods surveyed with a RMSD of 0.71 kcal mol<sup>-1</sup> (and 0.73 kcal mol<sup>-1</sup>), corresponding to chemical accuracy. The RMSDs are around 3 times smaller than that for CCSD. MP2, MP2.5, and MP3 overestimate the barrier heights in nearly all cases in the test set, with worst performances for the  $\text{HF} + \text{H} \longrightarrow \text{H}_2 + \text{F}$ ,  $\text{HF} + \text{H} \longrightarrow \text{H}_2 + \text{F}$ , and  $\text{OH} + \text{NH}_3 \longrightarrow \text{H}_2\text{O} + \text{NH}_2$  forward barriers, respectively. MP2.8: $\kappa$ -OOMP2 improves significantly on these cases with barrier height errors of 0.24 kcal mol<sup>-1</sup> and -0.51 kcal mol<sup>-1</sup>, respectively.

Assessment data for the NHTBH38<sup>57</sup> set are presented in Table 5. The NHTBH38 set

Table 4: Root mean square deviation, mean signed deviation, minimum deviation, and maximum deviation, in kcal mol<sup>-1</sup>, for the HTBH38 set.

Method	RMSD	MSD	MIN	MAX
CCSD	2.206	1.877	-0.782	4.146
MP2.8: $\kappa$ -OOMP2	0.711	-0.120	-1.424	1.301
MP3: $\kappa$ -OOMP2	0.730	0.346	-1.411	1.755
MP2.5	3.686	3.246	-0.273	7.323
MP3	3.883	3.506	0.695	7.214
$\kappa$ -OOMP2	2.918	1.658	-1.434	9.558
OOMP2	3.479	-0.952	-7.152	8.566
MP2	4.044	2.986	-1.487	12.142

contains forward and reverse barrier heights for 19 non-hydrogen transfer reactions. On this set, MP2.8: $\kappa$ -OOMP2 outperforms all other methods surveyed (RMSD of 0.76 kcal mol<sup>-1</sup>), with MP3: $\kappa$ -OOMP2 performing second best. The reduction in RMSD relative to MP3 is more than a factor of 8 for MP2.8: $\kappa$ -OOMP2. Remarkably, both methods improve substantially upon CCSD, with the improvement being more than a factor of 3 for MP2.8: $\kappa$ -OOMP2 MP2, MP2.5, and MP3 all exhibit large errors in the barrier heights for the reactions  $\text{H} + \text{N}_2\text{O} \longrightarrow \text{OH} + \text{N}_2$ ,  $\text{H} + \text{F}_2 \longrightarrow \text{HF} + \text{F}$ , and  $\text{CH}_3 + \text{ClF} \longrightarrow \text{CH}_3\text{F} + \text{Cl}$ . For  $\text{H} + \text{N}_2\text{O} \longrightarrow \text{OH} + \text{N}_2$  and  $\text{CH}_3 + \text{ClF} \longrightarrow \text{CH}_3\text{F} + \text{Cl}$ , both forward and reverse barriers are overestimated due to spin-contamination of the UHF reference for the transition state structures. The UHF reference  $\langle S^2 \rangle$  values of 1.011 and 1.026, respectively, are corrected to mean-field  $\langle S^2 \rangle$  values of 0.765 and 0.775, respectively, via the  $\kappa$ -OOMP2 orbital optimization procedure. For  $\text{H} + \text{F}_2 \longrightarrow \text{HF} + \text{F}$ , the reverse barriers are overestimated by more than 20 kcal mol<sup>-1</sup> with MP2, MP2.5, and MP3 while errors in the forward barriers are of similar magnitude to other systems in the data set. Significant spin-contamination is present in the UHF reference for both  $\text{F}_2$  and the transition state structure, leading to a cancellation of errors in the forward barrier that is not seen in the reverse barrier. Orbital optimization with  $\kappa$ -OOMP2 helps to mitigate this spin-contamination, reducing the mean-field  $\langle S^2 \rangle$  values of 0.293 and 1.212, respectively, to 0.000 and 0.767, respectively. For all three of these reactions MP2.8: $\kappa$ -OOMP2 gives errors that are reduced by a factor of 5-10 relative to MP2, MP2.5,

and MP3.

Table 5: Root mean square deviation, mean signed deviation, minimum deviation, and maximum deviation, in  $\text{kcal mol}^{-1}$ , for the NHTBH38 set.

Method	RMSD	MSD	MIN	MAX
CCSD	2.534	2.067	0.132	7.646
MP2.8: $\kappa$ -OOMP2	0.758	0.268	-0.949	1.579
MP3: $\kappa$ -OOMP2	1.668	1.076	-0.718	7.175
MP2.5	6.590	4.763	-0.328	24.455
MP3	6.651	5.158	1.099	23.283
$\kappa$ -OOMP2	2.766	1.553	-7.610	5.222
OOMP2	3.901	-1.650	-18.495	2.315
MP2	7.035	4.368	-2.676	25.627

To round out the test suite we assessed the performance of MP2.8: $\kappa$ -OOMP2 on two noncovalent interaction sets: the TA13 and A24 sets. The TA13 set contains 13 nonbonded interaction energies for radical closed-shell complexes.<sup>18</sup> We apply a counterpoise correction to these interaction energies to mitigate basis set superposition error (BSSE). Assessment data for the TA13 set is presented in Table 6. On this test set we see MP2.8: $\kappa$ -OOMP2 performs almost as well as CCSD. MP2.8: $\kappa$ -OOMP2 overbinds each interaction in the set, especially the  $\text{H}_2\text{O}$ -Al interaction which is overbound by  $2.05 \text{ kcal mol}^{-1}$ . Remarkably,  $\kappa$ -OOMP2 outperforms all methods surveyed on this set, with an RMSD of  $0.35 \text{ kcal mol}^{-1}$ . Table 7 presents the counterpoise-corrected results for the A24 set. The A24 set contains noncovalent interaction energies for 24 closed-shell small molecule complexes.<sup>59</sup> MP2.8: $\kappa$ -OOMP2 outperforms all other methods with a RMSD of  $0.08 \text{ kcal mol}^{-1}$  and a MSD of  $0.01 \text{ kcal mol}^{-1}$ . For the canonical MP methods, spin-contamination causes underbinding for the ethene-ethene and ethene-ethyne dimers. For the ethene dimer, the canonical MP errors are in excess of  $2 \text{ kcal mol}^{-1}$  while MP2.8: $\kappa$ -OOMP2 reduces this error to  $0.04 \text{ kcal mol}^{-1}$ .

Considering all the data presented, let us summarize the main conclusions obtained from this work.

1. At the MP2 level the choice of orbitals matters considerably, as is well known. In our work, for all 7 data sets considered, orbital optimized MP2 (OO-MP2) yields lower

Table 6: Root mean square deviation, mean signed deviation, minimum deviation, and maximum deviation, in kcal mol<sup>-1</sup>, for the TA13 set.

Method	RMSD	MSD	MIN	MAX
CCSD	0.722	0.539	-0.259	1.470
MP2.8: $\kappa$ -OOMP2	0.823	-0.459	-2.054	-0.011
MP3: $\kappa$ -OOMP2	0.808	-0.442	-2.463	0.086
MP2.5	1.559	0.276	-3.888	3.708
MP3	1.435	0.391	-2.612	3.997
$\kappa$ -OOMP2	0.350	-0.019	-0.589	0.650
OOMP2	0.789	-0.149	-1.938	1.370
MP2	1.791	0.160	-5.164	3.419

Table 7: Root mean square deviation, mean signed deviation, minimum deviation, and maximum deviation, in kcal mol<sup>-1</sup>, for the A24 set.

Method	RMSD	MSD	MIN	MAX
CCSD	0.247	0.226	0.093	0.429
MP2.8: $\kappa$ -OOMP2	0.075	0.007	-0.169	0.233
MP3: $\kappa$ -OOMP2	0.106	0.043	-0.113	0.373
MP2.5	0.492	0.132	-0.113	2.303
MP3	0.488	0.187	-0.010	2.203
$\kappa$ -OOMP2	0.184	-0.045	-0.631	0.199
OOMP2	0.193	-0.131	-0.475	0.063
MP2	0.515	0.078	-0.441	2.403

RMSD than MP2 (using unrestricted orbitals when necessary). Regularization via  $\kappa = 1.45$  has formal benefits in restoring Coulson-Fisher points. It also has practical benefits:  $\kappa$ -OOMP2 yields lower RMSD than OO-MP2 for all 7 data sets tested.

2. Use of  $\kappa$ -OOMP2 orbitals improves MP3 results to a surprising extent. MP3: $\kappa$ -OOMP2 has lower RMSD than MP3 by factors ranging from 1.7 to more than 5 across the 7 datasets reported here. MP3: $\kappa$ -OOMP2 is thus a far more robust method than MP3 itself, due to the reduced spin-contamination in  $\kappa$ -OOMP2 orbitals relative to HF orbitals.
3. Developing a semi-empirical variant based on scaling the MP2 and MP3 contributions yielded  $c_2 = 1.0$  and  $c_3 = 0.8$  based on the non-MR part of the W4-11 dataset (no regularization is preferred). In transferability tests, this MP2.8: $\kappa$ -OOMP2 method improves over MP3: $\kappa$ -OOMP2 in 4 of our 6 test sets, with the other two being very similar.
4. Remarkably, the results obtained with MP3: $\kappa$ -OOMP2 and MP2.8: $\kappa$ -OOMP2 produce lower RMSD than CCSD itself in 5 of the 7 datasets (the remaining two show no large failures). This indicates a level of performance that is beyond the physical content of MP3 theory, and involves some rather systematic cancellation of the effects due to connected triples.
5. These improved MP3 methods are single reference of course, and the datasets considered here are suitable for single reference methods. Much poorer performance must be expected for systems where strong correlations are in play (perhaps with the exception of biradicaloids<sup>19</sup>)

The improved performance granted by the use of  $\kappa$ -OOMP2 optimized orbitals suggests future developments in electronic structure theory. It will be interesting to assess results across additional data sets, and explore the use of larger basis sets. We intend to explore

scaled fourth-order perturbation approaches (MP4) and coupled cluster methods with  $\kappa$ -OOMP2 reference orbitals. The latter would be especially interesting in the context of nonvariational failures of CCSD(T). In a different direction, perhaps MP3 should be considered as an independent descriptor of electron correlation in double hybrid density functional theory, where MP2 is at present most widely used.<sup>27–31</sup>

## Acknowledgement

This work was supported by the U.S. Department of Energy, Office of Basic Energy Science, and Office of Advanced Scientific Computing Research through the SciDAC program.

## Supporting Information Available

The following files are available free of charge.

## References

- (1) Feyereisen, M.; Fitzgerald, G.; Komornicki, A. *Chem. Phys. Lett.* **1993**, *208*, 359 – 363.
- (2) Bernholdt, D. E.; Harrison, R. J. *Chem. Phys. Lett.* **1996**, *250*, 477 – 484.
- (3) Lochan, R. C.; Head-Gordon, M. *J. Chem. Phys.* **2007**, *126*, 164101.
- (4) Neese, F.; Schwabe, T.; Kossmann, S.; Schirmer, B.; Grimme, S. *J. Chem. Theory Comput.* **2009**, *5*, 3060–3073, PMID: 26609985.
- (5) Bozkaya, U.; Turney, J. M.; Yamaguchi, Y.; Schaefer, H. F.; Sherrill, C. D. *J. Chem. Phys.* **2011**, *135*, 104103.
- (6) Farnell, L.; Pople, J. A.; Radom, L. *J. Phys. Chem.* **1983**, *87*, 79–82.

(7) Nobes, R. H.; Pople, J. A.; Radom, L.; Handy, N. C.; Knowles, P. J. *Chem. Phys. Lett.* **1987**, *138*, 481 – 485.

(8) Gill, P. M. W.; Pople, J. A.; Radom, L.; Nobes, R. H. *J. Chem. Phys.* **1988**, *89*, 7307–7314.

(9) Jensen, F. *Chem. Phys. Lett.* **1990**, *169*, 519 – 528.

(10) Soydaş, E.; Bozkaya, U. *J. Chem. Theory Comput.* **2015**, *11*, 1564–1573, PMID: 26574366.

(11) Stück, D.; Head-Gordon, M. *J. Chem. Phys.* **2013**, *139*, 244109.

(12) Sharada, S. M.; Stück, D.; Sundstrom, E. J.; Bell, A. T.; Head-Gordon, M. *Mol. Phys.* **2015**, *113*, 1802–1808.

(13) Coulson, C. A.; Fischer, I. *Philos. Mag.* **1949**, *40*, 386–393.

(14) Razban, R. M.; Stück, D.; Head-Gordon, M. *Mol. Phys.* **2017**, *115*, 2102–2109.

(15) Lee, J.; Head-Gordon, M. *J. Chem. Theory Comput.* **2018**, *14*, 5203–5219, PMID: 30130398.

(16) Karton, A.; Daon, S.; Martin, J. M. *Chem. Phys. Lett.* **2011**, *510*, 165 – 178.

(17) Zipse, H. In *Radicals in Synthesis I*; Gansäuer, A., Ed.; Springer Berlin Heidelberg: Berlin, Heidelberg, 2006; pp 163–189.

(18) Tentscher, P. R.; Arey, J. S. *J. Chem. Theory Comput.* **2013**, *9*, 1568–1579, PMID: 26587618.

(19) Lee, J.; Head-Gordon, M. *arXiv e-prints* **2019**, arXiv:1903.11225.

(20) Lee, J.; Head-Gordon, M. *Phys. Chem. Chem. Phys.* **2019**, *21*, 4763–4778.

(21) Grimme, S. *J. Chem. Phys.* **2003**, *118*, 9095–9102.

(22) Jung, Y.; Lochan, R. C.; Dutoi, A. D.; Head-Gordon, M. *J. Chem. Phys.* **2004**, *121*, 9793–9802.

(23) Grimme, S. *J. Phys. Chem. A* **2005**, *109*, 3067–3077, PMID: 16833631.

(24) Lochan, R. C.; Jung, Y.; Head-Gordon, M. *J. Phys. Chem. A* **2005**, *109*, 7598–7605, PMID: 16834130.

(25) Distasio Jr., R. A.; Head-Gordon, M. *Mol. Phys.* **2007**, *105*, 1073–1083.

(26) Lochan, R. C.; Shao, Y.; Head-Gordon, M. *J. Chem. Theory Comput.* **2007**, *3*, 988–1003, PMID: 26627418.

(27) Grimme, S. *J. Chem. Phys.* **2006**, *124*, 034108.

(28) Chai, J.-D.; Head-Gordon, M. *J. Chem. Phys.* **2009**, *131*, 174105.

(29) Kozuch, S.; Martin, J. M. L. *Phys. Chem. Chem. Phys.* **2011**, *13*, 20104–20107.

(30) Mardirossian, N.; Head-Gordon, M. *J. Chem. Phys.* **2018**, *148*, 241736.

(31) Najibi, A.; Goerigk, L. *J. Phys. Chem. A* **2018**, *122*, 5610–5624, PMID: 29847940.

(32) Goldey, M.; Head-Gordon, M. *J. Phys. Chem. Lett.* **2012**, *3*, 3592–3598.

(33) Goldey, M.; Dutoi, A.; Head-Gordon, M. *Phys. Chem. Chem. Phys.* **2013**, *15*, 15869–15875.

(34) Goldey, M.; Head-Gordon, M. *J. Phys. Chem. B* **2014**, *118*, 6519–6525.

(35) Goldey, M. B.; Belzunces, B.; Head-Gordon, M. *J. Chem. Theor. Comput.* **2015**, *11*, 4159–4168.

(36) Hohenstein, E. G.; Parrish, R. M.; Martínez, T. J. *J. Chem. Phys.* **2012**, *137*, 044103.

(37) Grimme, S. *J. Comput. Chem.* **2003**, *24*, 1529–1537.

(38) Gráfová, L.; Pitoňák, M.; Řezáč, J.; Hobza, P. *J. Chem. Theory Comput.* **2010**, *6*, 2365–2376, PMID: 26613492.

(39) Riley, K. E.; Platts, J. A.; Řezáč, J.; Hobza, P.; Hill, J. G. *J. Phys. Chem. A* **2012**, *116*, 4159–4169, PMID: 22475190.

(40) Pitoňák, M.; Neogrády, P.; Černý, J.; Grimme, S.; Hobza, P. *ChemPhysChem* **2009**, *10*, 282–289.

(41) Riley, K. E.; Řezáč, J.; Hobza, P. *Phys. Chem. Chem. Phys.* **2012**, *14*, 13187–13193.

(42) Sedlak, R.; Riley, K. E.; Řezáč, J.; Pitoňák, M.; Hobza, P. *ChemPhysChem* **2013**, *14*, 698–707.

(43) Bozkaya, U. *J. Chem. Phys.* **2011**, *135*, 224103.

(44) Bozkaya, U.; Sherrill, C. D. *J. Chem. Phys.* **2014**, *141*, 204105.

(45) Bozkaya, U. *J. Chem. Theory Comput.* **2016**, *12*, 1179–1188, PMID: 26854993.

(46) Purvis, G. D.; Bartlett, R. J. *J. Chem. Phys.* **1982**, *76*, 1910–1918.

(47) Scuseria, G. E.; Janssen, C. L.; Schaefer, H. F. *J. Chem. Phys.* **1988**, *89*, 7382–7387.

(48) Raghavachari, K.; Trucks, G. W.; Pople, J. A.; Head-Gordon, M. *Chem. Phys. Lett.* **1989**, *157*, 479 – 483.

(49) Dunning, T. H. *J. Chem. Phys.* **1989**, *90*, 1007–1023.

(50) Kendall, R. A.; Dunning, T. H.; Harrison, R. J. *J. Chem. Phys.* **1992**, *96*, 6796–6806.

(51) Woon, D. E.; Dunning, T. H. *J. Chem. Phys.* **1993**, *98*, 1358–1371.

(52) Weigend, F.; Köhn, A.; Hättig, C. *J. Chem. Phys.* **2002**, *116*, 3175–3183.

(53) Hättig, C. *Phys. Chem. Chem. Phys.* **2005**, *7*, 59–66.

(54) Shao, Y. et al. *Mol. Phys.* **2015**, *113*, 184–215.

(55) Goerigk, L.; Grimme, S. *J. Chem. Theory Comput.* **2010**, *6*, 107–126, PMID: 26614324.

(56) Zhao, Y.; Lynch, B. J.; Truhlar, D. G. *Phys. Chem. Chem. Phys.* **2005**, *7*, 43–52.

(57) Zhao, Y.; González-García, N.; Truhlar, D. G. *J. Phys. Chem. A* **2005**, *109*, 2012–2018, PMID: 16833536.

(58) Goerigk, L.; Hansen, A.; Bauer, C.; Ehrlich, S.; Najibi, A.; Grimme, S. *Phys. Chem. Chem. Phys.* **2017**, *19*, 32184–32215.

(59) Řezáč, J.; Hobza, P. *J. Chem. Theory Comput.* **2013**, *9*, 2151–2155, PMID: 26583708.

# Graphical TOC Entry

